

# Radiative cascade of highly excited hydrogen atoms in strong magnetic fields

Türker Topçu and Francis Robicheaux

*Department of Physics, Auburn University, Alabama 36849-5311, USA*

(Received 17 August 2005; published 10 April 2006)

We have studied the radiative decay of atomic hydrogen in strong magnetic fields of up to 4 T. We have followed the radiative cascade from completely  $l, m$  mixed distributions of highly excited states as well as from distributions that involve highly excited states with  $|m| \sim n$ . We have found that the time it takes to populate the ground state is not affected by the magnetic field for the initial states with  $n \leq 20$ . For higher  $n$  manifolds, the electrons in the most negative  $m$  states are substantially slowed down by the magnetic field resulting in a much longer lifetime. We show that less than 10% of the antihydrogen atoms with  $n \sim 35$  generated in antihydrogen experiments at 4 K will decay to their ground states before they hit the wall of the vacuum container unless they are trapped. We have also found that the decay time is mainly determined by the fraction of atoms that were initially in highest negative  $m$  states due to the fact that only  $|\Delta m| + |\Delta \pi| = 1$  transitions are allowed in the magnetic field. We give a semiclassical method for calculating the decay rates for circular states and show that when the initial states have high- $|m|$ , semiclassical rates agree with the full quantum mechanical rates within a couple of percent for states with effective  $n \geq 20$ .

DOI: [10.1103/PhysRevA.73.043405](https://doi.org/10.1103/PhysRevA.73.043405)

PACS number(s): 32.80.Rm, 32.60.+i, 32.70.Cs

## I. INTRODUCTION

Formation of highly excited antihydrogen atoms have been reported by two experimental groups where cold antiprotons are merged with a cold trapped positron plasma at roughly [1] 16 K and [2,3] 4 K in magnetic fields of about 3 and 5.4 T, respectively. The goal is to perform Lorentz and *CPT* violation checks in the hyperfine spectrum of the  $2s \rightarrow 1s$  transition [4] for which the transition frequency is accurately known to about 1 part in  $10^{14}$  for atomic beam of hydrogen [5] and to about 1 part in  $10^{12}$  for trapped hydrogen [6]. The dominant process in the formation of the antihydrogen atoms is believed to be three body recombination [7] which yields a small fraction of antihydrogen atoms that are suitable for being laser stimulated down to the low- $n$  states [8]. It has also been noted that the antihydrogen atoms formed through three body recombination are likely to be in highly excited  $m$  states [9]. Since Lorentz and *CPT* violation experiments require ground state antihydrogen atoms, the highly excited antihydrogen atoms need to decay down to the ground state in order to serve this purpose. The knowledge of the decay rates and the time it takes to cascade down to the ground state from initial distributions of Rydberg states with  $|m| \sim n$  and from completely random  $l, m$  distributions of Rydberg states in strong magnetic fields are therefore necessary. We have investigated the radiative cascade from the Rydberg states with energies effectively corresponding to hydrogenic  $n$  manifolds of up to  $n=35$  in magnetic field strengths of up to 4.0 T. We have also followed the radiative cascade from these initial states in the presence of the black body radiation since the positron and antiproton plasmas have a temperature of 4 K in the case of the ATRAP experiment.

High- $|m|$  Rydberg atoms in the presence of strong magnetic fields were also investigated by Guest and Raithel [10]. They found that in case of the high- $|m|$  states in strong magnetic fields the motions that are parallel and transverse to the magnetic field are adiabatically separable. They studied the breakdown of the adiabaticity as they decreased

$|m|$  from 200 to 40 and observed that the motion in states with  $|m| \sim 200-80$  are adiabatically separable to the extent where no more than 50% of the energy levels are overtaken by the nonadiabatic couplings. As they decreased  $|m|$  further down to  $|m| \sim 40$  the energy spectrum experienced a transition from adiabaticity to nonadiabaticity. They have also calculated the natural and thermally enhanced decay rates for the states in which the motion is adiabatically separable [11]. In this paper, we perform calculations for the  $|m| \leq 40$  region which has not yet been treated.

In this study we also exploit the fact that the size of the positron and antiproton plasmas are small compared to the size of the trap. As a result, once an antihydrogen atom is formed, it quickly leaves the plasma and moves into the vacuum of the trap. If the antiatom is trapped then it spends its time in this vacuum radiatively decaying without positron-antiatom collisions. Therefore this study only considers radiative cascade in vacuum.

The radiative cascade from high Rydberg states exhibit interesting details. Reference [12] studied the phase space trajectory of an initial  $n, l$  state cascading to the ground state in zero magnetic field. In principle, a similar treatment using the quantum numbers in the magnetic field could be performed but is beyond the scope of this study.

We also give a semiclassical treatment for the radiative cascade from the highly excited circular Rydberg states for the sake of physical transparency. We have shown that the population time for the ground state strongly depends on the fraction of circular high- $|m|$  states in the initial distribution. We considered the relative effect of the cyclotron motion with respect to the magnetron motion in circular high- $|m|$  states on the decay rates and draw conclusions on the affinity of these states to magnetic field gradients.

All our calculations are for regular hydrogen rather than antihydrogen but the results apply equally well to antihydrogen. In this study, atomic units are used throughout unless stated otherwise.

## II. THEORY

Our results are obtained using an approximate Hamiltonian of a hydrogen atom placed in a magnetic field,

$$H = \frac{(\vec{p} - \vec{A}/c)^2}{2} - \frac{1}{r}, \quad (1)$$

where  $\vec{A}$  is the vector potential. In the Appendix we discuss the limitations of this Hamiltonian and show that it serves our purposes. With the choice of symmetric gauge  $\vec{A} = -\frac{1}{2}\vec{r} \times \vec{B}$  and a uniform magnetic field of magnitude  $B_0$  along the  $z$  direction, i.e.,  $\vec{B} = B_0\hat{z}$ , the Hamiltonian in spherical coordinates becomes

$$H = H_{\text{atom}} + \frac{\gamma}{2}L_z + \frac{\gamma^2}{8}r^2 \sin^2 \theta, \quad (2)$$

where  $H_{\text{atom}}$  is the atomic Hamiltonian in the absence of the magnetic field

$$H_{\text{atom}} = \frac{p^2}{2} - \frac{1}{r} \quad (3)$$

and  $\gamma = B_0/(2.35 \times 10^5 \text{ T})$  is the magnetic field strength in atomic units when  $B_0$  is in T. Note that the total Hamiltonian  $H$  has rotational symmetry about the  $z$  axis similar to the unperturbed atomic Hamiltonian.

In the next subsection, we describe the method used to compute the eigenenergy spectrum of the hydrogen atom in the magnetic field where we diagonalize the total Hamiltonian  $H$  in the basis spanned by the eigenstates of the atomic Hamiltonian  $H_{\text{atom}}$ . In the second subsection, we evaluate the dipole matrix elements in the magnetic field by rotating the dipole matrix elements calculated in the  $\{n, l, m\}$  basis into the dipole matrix elements in the  $\{m, \pi\}$  basis. The radiative decay rates in the magnetic field is then evaluated by using these rotated dipole matrix elements. In the last subsection, we solve the time dependent rate equation for an initial probability distribution of the eigenstates of  $H$ , which tells us how the initial probability distribution evolves in time.

### A. Calculation of the energy spectrum in the magnetic field

To calculate the new energy spectrum in the magnetic field, we diagonalized the matrix representation of the full Hamiltonian  $H$  in the basis spanned by the eigenstates  $\psi_{nlm}$  of the unperturbed atomic Hamiltonian. The matrix elements of the Hamiltonian  $H = H_{\text{atom}} + H_{\text{magnetic}}$  in this basis are

$$\begin{aligned} \langle nlm|H|n'l'm'\rangle &= \left[ \epsilon_{nl} + \frac{\gamma}{2}m \right] \delta_{n,n'} \delta_{l,l'} \delta_{m,m'} \\ &+ \frac{\gamma^2}{8} \langle nlm|r^2 \sin^2 \theta|n'l'm'\rangle, \end{aligned} \quad (4)$$

where  $\epsilon_{nl}$  are the eigenvalues of  $H_{\text{atom}}$ , i.e., energies of the hydrogen atom in the absence of the magnetic field. Noting that  $\sin^2 \theta = (2/3)[1 - \sqrt{4\pi/5}Y_2^0(\theta, \phi)]$ , the angular part of the last integral in Eq. (4) can be evaluated as

$$\begin{aligned} \langle lm|\sin^2 \theta|l'm'\rangle &= \frac{2}{3} \delta_{l,l'} \delta_{m,m'} - \frac{2}{3} (-1)^m \times \sqrt{(2l+1)(2l'+1)} \\ &\times \begin{pmatrix} l & 2 & l' \\ 0 & 0 & 0 \end{pmatrix} \begin{pmatrix} l & 2 & l' \\ -m & 0 & m' \end{pmatrix}. \end{aligned} \quad (5)$$

Selection rules for these matrix elements can be deduced from the fact that the 3- $j$  symbols must satisfy the triangle relations (Ref. [16]) simultaneously in order to survive. For the 3- $j$  symbols involved in Eq. (5), this condition is realized as  $|l-l'| \leq 2$ . Also the survival of the first 3- $j$  symbol in Eq. (5) requires that the sum of the elements on the first row must be an even integer. This condition along with  $|l-l'| \leq 2$  implies that the magnetic field will only induce transitions for which  $\Delta l = 0$  or  $\Delta l = \pm 2$ . Therefore with the definition

$$R_{n',l'}^{n,l}(\eta) = \int R_{n,l}(r) r^\eta R_{n',l'}(r) dr, \quad (6)$$

where  $R_{n,l}(r)$  is the radial part of the eigenfunction  $\psi_{nlm}$ , the matrix elements of the full Hamiltonian  $H$  in the  $\{nlm\}$  basis become

$$\begin{aligned} \langle nlm|H|n'l'm'\rangle &= \left[ \epsilon_{nl} + \frac{\gamma}{2}m \right] \delta_{n,n'} \delta_{l,l'} \delta_{m,m'} + \frac{\gamma^2}{12} \\ &\times \left[ \delta_{m,m'} \delta_{l,l'} - (-1)^m \sqrt{(2l+1)(2l'+1)} \right. \\ &\times \left. \begin{pmatrix} l & 2 & l' \\ 0 & 0 & 0 \end{pmatrix} \begin{pmatrix} l & 2 & l' \\ -m & 0 & m' \end{pmatrix} \right] R_{n',l'}^{n,l}(2). \end{aligned} \quad (7)$$

Here  $R_{n,l}(r)$  is generated on a square root mesh by direct integration of the Schrödinger equation in a box. All orbitals satisfy the boundary condition such that  $R_{n,l}(r_f) = 0$ , where the box size  $r_f$  is chosen to be larger than the size of the physical states in our simulations. By choosing this boundary condition, we greatly increase the rate of convergence with  $n$  because eigenenergies  $\epsilon_{nl}$  increase rapidly with  $n$  for large  $n$  [13]. Thus our basis has substantial continuum character.

We have checked the convergence of our results with respect to the box size  $r_f$ , the number of radial grid points  $N$  and the  $n_{\text{max}}$  and  $l_{\text{max}}$  describing the basis set used in the diagonalization of  $H$ . For example, in a 4.0 T field, decay times obtained for  $n=30$  in a 2000 a.u. box with 8000 radial points using a basis with  $(n_{\text{max}}, l_{\text{max}}) = (45, 40)$  differ from the decay times obtained in a 3000 a.u. box with 12 000 points using a basis described by  $(n_{\text{max}}, l_{\text{max}}) = (50, 45)$  at a few percent level. The energy of the state  $(n_{\text{max}}, 0)$  in the 2000 a.u. box is  $\epsilon_{45,0} = 4.1138 \times 10^{-4}$  a.u. and the energy of the state  $(30, 0)$  is  $\epsilon_{30,0} = -5.5526 \times 10^{-4}$  a.u. For the 3000 a.u. box the state with  $(n_{\text{max}}, 0)$  has the energy  $\epsilon_{50,0} = 3.8628 \times 10^{-5}$  a.u. whereas energy of the state  $(30, 0)$  is the exact value  $-5.5556 \times 10^{-4}$  a.u.

Diagonalization of the matrix with the matrix elements given by Eq. (7) gives the new energy spectrum  $\{\tilde{\epsilon}_j\}$  of the hydrogen atom in the magnetic field. Note that in the presence of the magnetic field the good quantum numbers are the

magnetic quantum number  $m$  and the  $z$  parity  $\pi$  rather than the principal quantum number  $n$  and the orbital quantum number  $l$ .

As a check on our codes, we have compared our energies for hydrogenic  $n=23$  manifold in a 4.7 T field for states with  $m=0, 1, 2$  listed in Ref. [14] and found very good agreement except at a few particular energy values. The difference might be due to the fact that nonorthogonal basis set methods, similar to the one used in Ref. [14], can be unstable, e.g., their energies may not be converged for those particular states.

### B. Calculation of the dipole matrix elements

To calculate the dipole matrix elements in the magnetic field, we first calculated the dipole matrix elements in the  $\{nlm\}$  basis and rotated those matrix elements obtaining the dipole matrix elements in the  $\{m\pi\}$  basis of the full Hamiltonian  $H$ .

Dipole matrix elements for the linearly polarized states in the  $\{nlm\}$  basis are

$$\langle nlm|z|n'l'm'\rangle = \langle nl|r|n'l'\rangle \langle lm|\cos\theta|l'm'\rangle. \quad (8)$$

Again noting that  $\cos\theta = \sqrt{4\pi/3}Y_1^0(\theta, \phi)$  one can deduce

$$\begin{aligned} \langle nlm|z|n'l'm'\rangle &= (-1)^m \sqrt{(2l+1)(2l'+1)} \times \begin{pmatrix} l & 1 & l' \\ 0 & 0 & 0 \end{pmatrix} \\ &\times \begin{pmatrix} l & 1 & l' \\ -m & 0 & m' \end{pmatrix} R_{n',l'}^{n,l}(1). \end{aligned} \quad (9)$$

In the same manner, for the left and right hand circularly polarized states one obtains

$$\begin{aligned} \left\langle nlm \left| \frac{x \pm iy}{\sqrt{2}} \right| n'l'm' \right\rangle &= \mp (-1)^m \sqrt{(2l+1)(2l'+1)} \\ &\times \begin{pmatrix} l & 1 & l' \\ 0 & 0 & 0 \end{pmatrix} \\ &\times \begin{pmatrix} l & 1 & l' \\ -m & \pm 1 & m' \end{pmatrix} R_{n',l'}^{n,l}(1) \end{aligned} \quad (10)$$

respectively. Selection rules for the magnetic field induced transitions can be deduced from the properties of the 3- $j$  symbols in Eqs. (9) and (10) as before. Since the second row of the second 3- $j$  symbols in both of the expressions need to add up to zero for the survival of the term, we can immediately conclude that there is no  $m$  change for the linearly polarized states while the circularly polarized states change  $m$  by 1. Also the first 3- $j$  symbols in the terms tell us that  $|l-l'| \leq 1$  and  $|l+l'|$  must be an odd integer implying that  $l$  must change by one for the term to survive. Since  $l_{\min} = m + \pi$  and  $l$  increases from  $l_{\min}$  to  $n-1$  in integer steps for a given  $m$ , it can be concluded that  $|\Delta m| + |\Delta \pi| = 1$  for an allowed transition.

To obtain the dipole matrix elements in  $\{m\pi\}$  space, we simply rotate the matrix elements in Eqs. (9) and (10) computed in the  $\{nlm\}$  basis. Let us index the state  $(nlm)$  by  $j$  and the state  $(m\pi)$  by  $\alpha$ . Denoting the new rotated dipole matrix element by  $d_{\alpha,\alpha'}$  we have

$$d_{\alpha,\alpha'} = \sum_j \sum_{j'} \langle \psi_j | d | \psi_{j'} \rangle U_{j,\alpha}^* U_{j',\alpha'}, \quad (11)$$

where  $d$  is the dipole operator which is  $z$  for linearly polarized states and  $(x \pm iy)/\sqrt{2}$  for the left and right hand circularly polarized states, respectively. The rotation matrix  $U$  is the matrix whose columns are the eigenvectors of the full Hamiltonian  $H$  in the  $\{nlm\}$  basis which is obtained by direct diagonalization of  $H$ ,

$$\sum_j H_{kj} U_{j\alpha} = U_{k\alpha} \tilde{\epsilon}_\alpha \quad (12)$$

where  $\tilde{\epsilon}_\alpha$  is the  $\alpha$ th eigenenergy of the Hamiltonian  $H$  with the eigenstate  $U_\alpha$ .

Having obtained the dipole matrix elements we now can calculate the partial decay rates of the states of the hydrogen atom in the magnetic field. Partial decay rate from initial state  $i$  to final state  $f$  in length gauge is given by

$$\Gamma_{fi} = \frac{4}{3c^3} (\tilde{\epsilon}_i - \tilde{\epsilon}_f)^3 |\langle \tilde{\psi}_f | \vec{r} | \tilde{\psi}_i \rangle|^2, \quad (13)$$

where  $\tilde{\epsilon}_\alpha$  and  $\tilde{\psi}_\alpha$  are the energy and the eigenfunction of state  $\alpha$  of the hydrogen atom in the magnetic field and  $4/(3c^3) = 5.181 \times 10^{-7}$  in atomic units. Note that the usual velocity gauge expression derived in the absence of a magnetic field becomes

$$\Gamma_{fi} = \frac{4}{3c^3} (\tilde{\epsilon}_i - \tilde{\epsilon}_f) |\langle \tilde{\psi}_f | \vec{p} - \vec{A}/c | \tilde{\psi}_i \rangle|^2 \quad (14)$$

with the inclusion of the magnetic field because the physical momentum of the electron is now  $(\vec{p} - \vec{A}/c)$  as being different from the canonical momentum  $\vec{p}$  of the electron.

### C. Solution of the rate equation

Having obtained the partial decay rates  $\Gamma_{\alpha,\alpha'}$  in the magnetic field, we solved the time dependent rate equation to simulate the flow of initial probability distribution among the states. The rate equation for the probability  $\wp_\alpha$  of finding the atom in state  $\alpha$  is

$$\frac{d\wp_\alpha}{dt} = -\Gamma_\alpha \wp_\alpha + \sum_{\alpha' > \alpha} \Gamma_{\alpha'\alpha} \wp_{\alpha'}, \quad (15)$$

where  $\Gamma_\alpha$  is the total decay rate of state  $\alpha$ ,

$$\Gamma_\alpha = \sum_{\alpha' < \alpha} \Gamma_{\alpha'\alpha}. \quad (16)$$

Note that the condition  $\alpha > \alpha'$  implies the constraint  $\tilde{\epsilon}_{\alpha'} < \tilde{\epsilon}_\alpha$ . The first term on the right hand side of the rate equation represents the total flow of probability out of the state  $\alpha$  while the sum in the second term is due to the total flow of probability into state  $\alpha$  from all higher states  $\alpha'$ . The  $\Gamma_{\alpha,\alpha'}$  span several orders of magnitude making Eq. (15) difficult to solve. Assume the solution to be of the form  $\wp_\alpha = \wp_\alpha^{(0)} + \wp_\alpha^{(1)}$  where  $\wp_\alpha^{(0)}$  satisfies

$$\frac{d\varphi_\alpha^{(0)}}{dt} = -\Gamma_\alpha \varphi_\alpha^{(0)}. \quad (17)$$

The time propagation of this equation by one time step  $\delta t$  for a given  $\varphi_\alpha^{(0)}$  at a time  $t$  is

$$\varphi_\alpha^{(0)}(t + \delta t) = e^{-\Gamma_\alpha \delta t} \varphi_\alpha^{(0)}(t). \quad (18)$$

Substituting  $\varphi_\alpha = \varphi_\alpha^{(0)} + \varphi_\alpha^{(1)}$  into the rate equation and noting that  $\sum_{\alpha'} \varphi_{\alpha'}^{(0)}(0) = \sum_{\alpha'} \varphi_{\alpha'}^{(1)}(0) = 1$ , one obtains

$$\varphi_\alpha^{(1)}(t + \delta t) = \sum_{\alpha' > \alpha} B_{\alpha\alpha'} (1 - e^{-\Gamma_{\alpha'} \delta t}) \varphi_{\alpha'}^{(0)}(t), \quad (19)$$

where  $B_{\alpha\alpha'} \equiv \Gamma_{\alpha\alpha'}/\Gamma_{\alpha'}$  is the branching ratio. Combining Eqs. (18) and (19)  $\varphi_\alpha$  becomes

$$\varphi_\alpha(t + \delta t) = e^{-\Gamma_\alpha \delta t} \varphi_\alpha^{(0)}(t) + \sum_{\alpha' > \alpha} B_{\alpha\alpha'} (1 - e^{-\Gamma_{\alpha'} \delta t}) \varphi_{\alpha'}^{(0)}(t). \quad (20)$$

For an initial distribution of probability among the states one can propagate the probability distribution along time with the knowledge of the decay rates. We have checked the convergence of our results with respect to the maximum effective cut off quantum numbers  $n_c, l_c$  of the basis states used to describe the radiative decay from a given initial distribution. The states that make up this initial distribution have effective quantum numbers that are smaller than these cut off  $n_c, l_c$  quantum numbers. Convergence with respect to the time step  $\delta t$  was also checked.

### III. RESULTS

We will start by making some rough estimates for the effect of the magnetic field on the classical velocity of the electron in a circular orbit to obtain an idea of the extent to which the decay rates from these states change from their field free estimates. The second subsection contains results from calculations for the radiative cascade in 1.0, 2.0, 3.0, and 4.0 T fields where the initial distribution of states with energies corresponding to various principal quantum numbers up to  $n=35$  are completely  $l, m$  mixed. These results are compared with some results obtained using an analytical rate formula. In the following subsection we present results from calculations for which the initial states are localized in the highest  $|m|$  regions of an  $n$  manifold and again some results obtained using an analytical formula for the decay rates. The effect of the black body radiation will be taken into account to see if the results of the previously presented radiative cascade calculations are affected by a 4 K [2,3] radiation field. Finally we present a semiclassical treatment for the calculation of the radiative decay rates of circular orbits and compare them to those calculated quantum mechanically.

#### A. Rough estimates

For a classical electron in a closed circular orbit in a Coulomb field, Newton's laws give

$$m_e \frac{v_0^2}{r} = k \frac{e^2}{r^2}, \quad (21)$$

where we have employed the SI units. Solution of this equation for the classical velocity immediately yields  $v_0 = \pm \sqrt{ke^2/m_e r}$ . In the presence of a uniform magnetic field of strength  $B_0$  directed perpendicular to the plane of the circular orbit, Eq. (21) becomes

$$m_e \frac{v^2}{r} = k \frac{e^2}{r^2} + evB_0 \quad (22)$$

whose direct solution for  $v$  now yields

$$v = \frac{eB_0 r}{2m_e} \pm \sqrt{\left(\frac{eB_0 r}{2m_e}\right)^2 + v_0^2}. \quad (23)$$

Note that the  $\pm$  sign in front of the square root term in Eq. (23) implies the fact that electron either speeds up or slows down depending on the sign of  $L_z$  for a given direction of the magnetic field. Expanding the square root to the fourth order in binomial series for the case  $eB_0 r/(2m_e) < v_0$ , one approximates the classical velocity in magnetic field  $v$  by

$$v \approx \frac{eB_0 r}{2m_e} \pm \left[ v_0 + \frac{1}{2v_0} \left(\frac{eB_0 r}{2m_e}\right)^2 + \frac{1}{8v_0^3} \left(\frac{eB_0 r}{2m_e}\right)^4 \right]. \quad (24)$$

Noting that  $k=m_e=e=1$  in atomic units and  $r \sim n^2$  for a circular classical orbit with energy  $\epsilon \sim -1/(2n^2)$ , we can infer

$$v_n^{\text{cl}} \approx \pm \frac{1}{n} \left[ 1 \mp \frac{\gamma n^3}{2} + \frac{1}{8} (\gamma n^3)^2 + \frac{1}{128} (\gamma n^3)^4 \right], \quad (25)$$

where we have recalled that  $\gamma = B_0/(2.35 \times 10^5 \text{ T})$  is the magnetic field in atomic units when  $B_0$  is in T.

In the field free case, Eq. (25) predicts  $v_n^{\text{cl}} \approx 1/n$  for all  $n$  which is exactly the quantum mechanical velocity  $v_n = 1/n$ . For  $n=10$ , the zero field velocity differs from the  $B_0=4.0$  T value by  $\sim 1\%$ . At  $n=20$  the difference between the velocities for 2.0 T field and the zero field is  $\sim 3\%$  and  $\sim 7\%$  at 4.0 T. When we are up to  $n=30$ ,  $v_n^{\text{cl}}$  differs from zero field value by  $\sim 12\%$  for  $B_0=2.0$  T, by  $\sim 19\%$  for  $B_0=3.0$  T, and by  $\sim 26\%$  for  $B_0=4.0$  T. This suggests that magnetic field strengths of interest in the anti-hydrogen experiments has little effect on the circular orbits with  $n < 10$  while starting to effect the velocities in the orbits with  $n \sim 20$  within  $\sim 10\%$  and in the orbits with  $n \sim 30$  within  $\sim 30\%$ . Noting that the radiative decay rate scales like  $a^2 \sim v^4/r^2$ , we can infer that the magnetic field affects the decay rates more strongly than it affects the velocity of the electron in the orbit.

In the limit where  $eB_0 r/2m_e \gg v_0$  Eq. (23) can be expanded to second order as

$$v_n^{\text{cl}} \approx \frac{eB_0 r}{2m_e} \pm \frac{eB_0 r}{2m_e} \left( 1 + \frac{v_0^2}{2(eB_0 r/2m_e)^2} \right) \quad (26)$$

yielding  $v_+^{\text{cl}} \approx eB_0 r/m_e + v_0^2/(eB_0 r/m_e)$  for the orbit in which the electron is sped up, and  $v_-^{\text{cl}} \approx -v_0^2/(eB_0 r/m_e)$  for the orbit in which the electron is slowed down by the magnetic field. The case where the electron is slowed down corresponds to the guiding center approximation since the Larmor period is



much smaller than the orbital period of the electron. In 4.0 T field, the absolute value of the ratio of the velocities in orbits with same energy but of opposite helicities, i.e.,  $|v_+^{cl}/v_-^{cl}|$ , is  $\approx 1$  for orbits with  $n$  up to 25,  $\sim 1.2$  at  $n=30$ , and  $\sim 2.2$  at  $n=40$ .

### B. Energy spectrum in the magnetic field

From the diagonalization of the full Hamiltonian  $H$ , we have found that the energies of the states with negative magnetic quantum numbers decrease whereas the energies of the states with positive magnetic quantum numbers increase with the increasing magnetic field strength. In the antihydrogen experiments, magnetic field will be deliberately generated in such a way that it is stronger near the walls of the cylindrical container in which antiproton and positron plasmas are mixed. Therefore the states with negative  $m$ 's are attracted by the increasing magnetic field strength and states with positive  $m$ 's are repelled by the increasing magnetic field. Hence we can expect the states with negative  $m$  that are close to the magnetic field gradient to plummet to the wall of the container faster than those with positive  $m$ . Therefore atoms that are formed with high field seeking character will need to decay especially rapidly if they are not to be accelerated by the magnetic field gradients. For extremely negative  $m \sim -200$  of Ref. [11], the atoms could have low field seeking character because the positive magnetic moment from the electron's cyclotron motion is larger in magnitude than the negative magnetic moment from the guiding center character of the electron's motion around the proton.

### C. Radiative cascade starting from completely random ( $l, m$ ) distribution

Since  $n$  is not a good quantum number when magnetic field is present, the initial probability distribution was chosen such that the probability of finding the atom in a state whose energy is between energies of hydrogenic  $n$  and  $n-1$  manifolds is equally partitioned between the states that lay in this energy range. Initial distributions that correspond to  $n=10, 15, 20, 25, 30$ , and  $35$  in magnetic fields of strengths 1.0, 2.0, 3.0, and 4.0 T have been explored. Furthermore, instead of monitoring the flow of probability of finding the atom within a particular state, we have monitored the probability of finding the atom in a state whose energy lies in a range which embraces  $5-10 n$  manifolds. Evolution of the probability distribution with time when started out in states with effective  $n=35$  in a 4.0 T field are plotted in Fig. 1. As time progresses, states of lower energies become populated, eventually with all population ending up in the ground state. At early times the fast decay is mostly coming from the low- $|m|$  states which cascade by large  $\Delta n$  steps. The slow decay at later times is due to the states with large- $|m|$  which cascade through  $\Delta n \sim -1$  transitions.

In the antihydrogen experiments, the formed antihydrogen atoms move through a magnetic field that is spatially dependent, e.g., stronger near the walls of the cylindrical container. Since the magnetic force on the center of mass of the antihydrogen atom depends on its internal energy, it is important to know the time scale for the variation of the internal energy

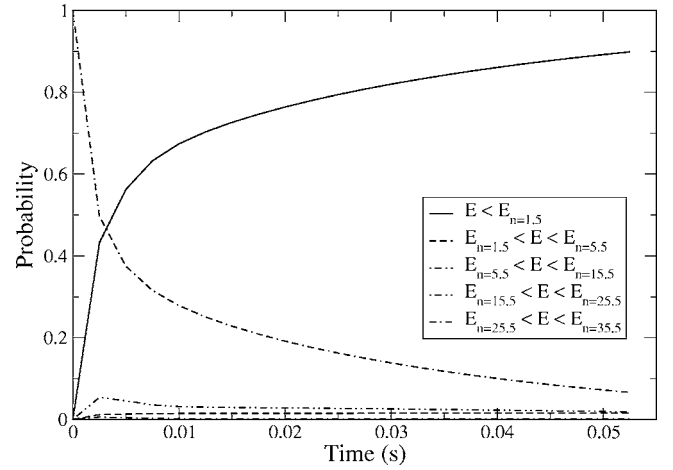


FIG. 1. Flow of probability in the completely  $l, m$  mixed distribution for  $n=35$  in a 4.0 T field as a function of time. Each curve represents the total probability of finding the atom in a state whose energy is in one of the particular energy ranges indicated on the legend.

of the antihydrogen atom to estimate the time it has before colliding with the wall of the container and get annihilated. A practical percentage of the antiatoms should decay to the ground state before they get destroyed to be used in the *CPT* and Lorentz violation experiments. Therefore we have calculated the time it would take to populate the ground state by 10, 20, 50, and 90% if everything starts from states that are in the aforementioned  $n$  regimes. In Figs. 2(a) and 2(b) the time it takes 10 and 50% of the hydrogen atoms to decay

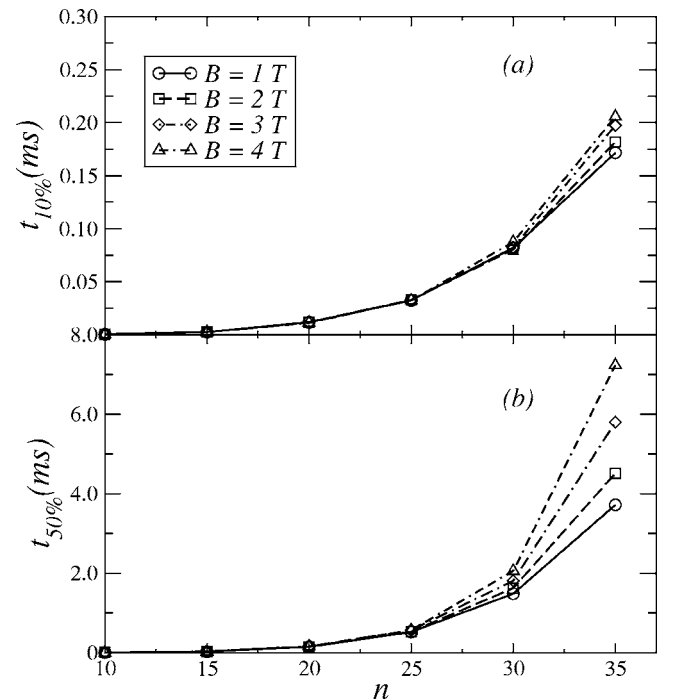


FIG. 2. Time required to populate the ground state of the hydrogen atom by (a) 10 and (b) 50% as a function of the effective hydrogenic principal quantum number  $n$  for 1.0, 2.0, 3.0, and 4.0 T fields. Initial distribution of states is completely  $l, m$  mixed.

down to the ground state as a function of the given initial state  $n$  is plotted for four different magnetic field strengths. It can be seen that for  $n \lesssim 25$  the magnetic field makes no important difference in terms of populating the ground state by 10% and when we are up to  $n=35$  we see  $\sim 0.4$  ms separation between 1.0 and 4.0 T values. This implies that the increase in the time it takes to populate the ground state by  $n$  is mainly a zero field effect. When we look at the 50% population plot it can be noted that for  $n \lesssim 25$  there is no change coming from increasing the field strength but by  $n=30$  there is  $\sim 0.8$  ms and by  $n=35$  there is  $\sim 3.5$  ms separation between the lowest and highest magnetic field strengths.

The thermal speed  $\sqrt{k_B T/M}$  of an antihydrogen atom at 4 K [2,3] is  $\sim 260$  m/s which is  $\sim 26$  cm/ms and higher by a factor of 2 at 16 K [1]. Noting that the diameter of the cylindrical container is approximately a couple of centimeters, we can conclude that in the field regime of the experiments there is not enough time to populate the ground state by even 50% before the antihydrogen atoms hit the walls and get destroyed. According to Fig. 2(a), for  $n=35$  the time needed to populate the ground state by 10% is about 0.2 ms in which the thermal antihydrogen atoms can move  $\sim 6$  cm. Hence we can conclude that at 4 K and in magnetic fields up to  $\sim 4$  T the ground state population will not be able to exceed 10%. Since ATHENA experiment runs at a higher temperature, this population percentage would be even lower in their experiment. It seems clear that in order to trap substantial amounts of antihydrogen, the antiatoms need to be trapped while in Rydberg states.

Since the lifetime of the completely  $l, m$  mixed case increases  $\sim n^5$  for a highly excited hydrogenic state in the absence of a magnetic field, time scaled by  $n^5$  would stay roughly constant as  $n$  increases. Therefore we scaled our results for the decay times by  $n^5$  to see the  $n$  range for which decay times are practically unaffected by the magnetic field. These scaled plots can be seen in Fig. 3 where we have plotted scaled time needed for the ground state to be populated by 10, 50, and 90% versus initial  $n$ . In all the plots, scaled time stays approximately constant up until  $n \sim 25$  meaning that decay rates of these states are not affected by the magnetic field compared to the field free case; this is due to the fast direct decay to low  $n$ -states. Scaled time then starts to spread out noticeably with growing  $n$  there on. The states with higher- $|m|$  decay more slowly and have rates that are more strongly affected by the magnetic field. This is the reason for the larger magnetic field effect in Figs. 3(b) and 3(c) than in Fig. 3(a).

For comparison, we have also done the same calculations for zero field case using decay rates calculated via an analytical formula which assumes complete  $l$  mixing of the states populated in the initial distribution when there is no magnetic field [16]. In the actual decay process, states with low- $|m|$  can make bigger  $\Delta n$  jumps towards the ground state than the ones with high- $|m|$ , resulting in the pile up of population in states with  $|m| \sim n$  over time. Since the analytical formula assumes complete  $l$  mixing within individual  $n$  manifolds, it does not simulate the actual behavior after the piling up of population in high- $m$  states. Therefore the applicability of this analytical formula is limited to short time periods from the beginning. In this picture, partial decay rate from state  $n_i$  to state  $n_f$  is

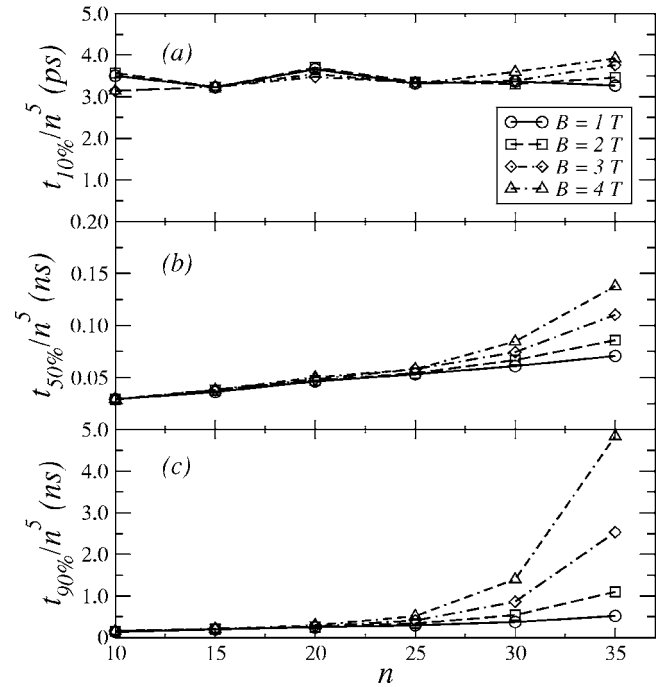


FIG. 3. Scaled time required to populate the ground state of the hydrogen atom by (a) 10, (b) 50, and (c) 90% as a function of the effective hydrogenic principal quantum number  $n$  for 1.0, 2.0, 3.0, and 4.0 T fields. Initial distribution of states is completely  $l, m$  mixed.

$$\Gamma_{n_i \rightarrow n_f} = \frac{8\alpha^3}{3\sqrt{3}\pi} \frac{1}{n_i^5 n_f} \frac{1}{1 - (n_f^2/n_i^2)}, \quad (27)$$

where  $\alpha$  is the fine structure constant. The total decay rate is again calculated as usual,

$$\Gamma_{n_i} = \sum_{n_f=1}^{n_i-1} \Gamma_{n_i \rightarrow n_f}. \quad (28)$$

For  $n=20$ , time needed for population of the ground state to reach 10% is calculated using the rates from Eq. (27) is about 27% bigger than our quantal result while 90% population result is off by about 60%. Going up to  $n=30$  we found that time for 10% population of the ground state is longer by  $\sim 14\%$  and 90% population time is longer by  $\sim 76\%$  than our quantum mechanical result.

#### D. Radiative cascade starting from high- $|m|$ distribution

The dominant process in the antihydrogen formation is believed to be three-body recombination. It is also known that the atoms formed in this process are likely to be in a high  $m$  state [9]. This is clearly a different situation than the completely  $l, m$  mixed case where every state within a prescribed energy range is equally likely to be populated. To simulate the case of the three-body recombination, we restricted our initial states not just being in the  $[\epsilon_{n-1}, \epsilon_n]$  energy range but also their  $m$  values to be extreme to qualify as one of the initial states. We investigated both extreme cases in which  $m \sim n$  and  $m \sim -n$  although it seems that the  $m \sim -n$

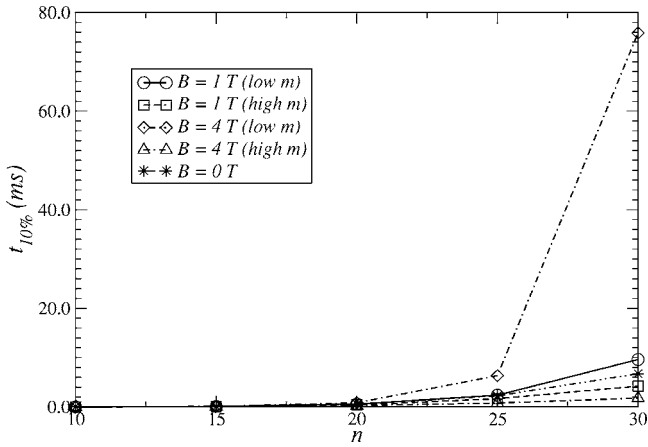


FIG. 4. Time required to populate the ground state of the hydrogen atom by 10% as a function of the effective hydrogenic principal quantum number  $n$  for 1.0 and 4.0 T fields. Initial distribution of states only involves states with high  $|m|$ .

case is more likely. High- $|m|$  states are chosen such that there are only a few states that make up the initial distribution.

For comparison, we also calculated the time it takes the atom to reach its ground state in zero magnetic field by an approximate formula for the decay of circular states

$$\Gamma_{n \rightarrow (n-1)} = \frac{2}{3 \left( n - \frac{1}{2} \right)^2 n^3 c^3}. \quad (29)$$

The decay rate estimates we made using Eq. (29) for zero magnetic field are in agreement with the exact quantum results within about 5% for the states with  $n=2$  and get better with increasing  $n$  reaching agreement with the quantal result within 0.5% by  $n=5$  for  $B_0=0$ .

The results of the quantum mechanical calculations for 10% population of the ground state are plotted in Fig. 4 for magnetic field strengths of 1.0 and 4.0 T for highest and lowest  $m$  states in their respective  $n$  manifolds with the zero field results for comparison. Both 1.0 and 4.0 T curves for high  $m$  lie just below the zero field results throughout the whole  $n$  range from 10 to 30, while for the states with lowest  $m$ 's 1.0 T field lifts the 10% population time just above the zero field curve and 4.0 T field stretches the required time for 10% population of the ground state from the zero field value by a factor of  $\sim 13$  for  $n=30$ . Note that the largest effect is for the states with  $m \sim -n$ , only becoming important above  $n \sim 25$ . The fact that the 4.0 T field has a more pronounced effect for the  $|m| \sim -n$  mixed distribution than for the completely  $l, m$  mixed distribution is because now the states in the distribution are mostly circular and most of the transitions are of  $\Delta n = -1$  type.

In Fig. 5, the times required for the population of the ground state by 10, 50, and 90% are scaled by  $n^6$  since now initial distribution involves only circular states. Scaled decay times are plotted versus  $n$  for the high- $|m|$  states again in magnetic fields of strengths 1.0 and 4.0 T. In all three plots,

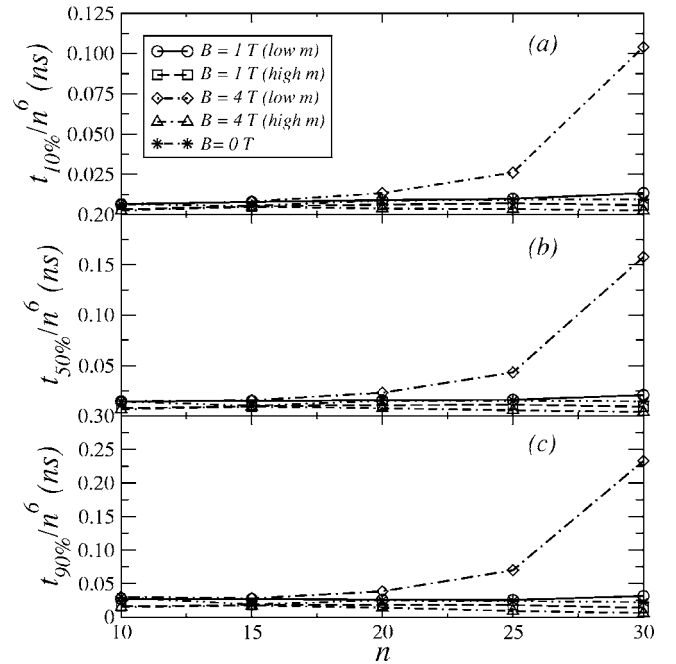


FIG. 5. Scaled time required to populate the ground state of the hydrogen atom by (a) 10, (b) 50, and (c) 90% as a function of the effective hydrogenic principal quantum number  $n$  for 1.0 and 4.0 T fields. Initial distribution of states only involves states with  $|m| \sim n$ .

both of the  $m \sim n$  cases lie just below the zero field curve. For the states with  $m \sim -n$ , 1.0 T field cannot alter the scaled time of 10% population by more than  $\sim 30\%$  from the field free case but for the 4.0 T field scaled population time is larger than zero field case by a factor of  $\sim 2.5$  at  $n=25$  and by a factor of  $\sim 11$  by  $n=30$ . Again starting from the states with  $m \sim -n$ , 50% population of the ground state in 1.0 T field does not differ from the field free value by more than  $\sim 25\%$  but for the 4.0 T field scaled population time is larger than zero field case by a factor of  $\sim 3$  at  $n=25$  and by a factor of  $\sim 11$  by  $n=30$ . For the 90% population of the ground state, 1.0 T field again does not do a good job in lifting the scaled time by  $n \sim 25$  from the zero field value and the 4.0 T field again gives higher scaled time than zero field by a factor of  $\sim 2.5$  at  $n=25$  and by a factor of  $\sim 15$  at  $n=30$ . The fact that the decay time for the negative  $m$ -states is much longer than the positive  $m$ -states can be understood from classical arguments. The classical radiation is proportional to the square of the acceleration of the electron which goes  $\sim v^2/r$ . Since the electrons in states with  $m \sim -n$  are slowed down by the magnetic field, they have lower acceleration than the electrons in states with  $m \sim n$ . Therefore the electrons in states with  $m \sim -n$  radiate less intensely and decay more slowly compared to the electrons in states with  $m \sim n$ .

### E. Effect of black body radiation

One concern was whether the experimentally reported black body temperatures of 16 K [1] and 4 K [2,3] could strongly affect the radiative decay rates. The effect would be

stimulated emission and photoabsorption fueled by the black body radiation. Expressing the decay rates in terms of Einstein  $A$  and  $B$  coefficients, the rate of radiative decay from state  $i$  to state  $f$  would be

$$A_{i \rightarrow f} + B_{i \rightarrow f} u(\nu_{if}), \quad (30)$$

where  $u(\nu_{if})$  is the Planck distribution

$$u(\nu_{if}) = \frac{\hbar \omega^3}{\pi^2 c^3} \frac{1}{e^{h\nu_{if}/k_B T} - 1}. \quad (31)$$

Einstein  $B_{i \rightarrow f}$  coefficient is evaluated from the  $A_{i \rightarrow f}$  coefficient in the following manner:

$$B_{i \rightarrow f} = \frac{\pi^2 c^3}{\hbar \omega^3} A_{i \rightarrow f}. \quad (32)$$

In terms of evaluating the effect of the black body radiation, an important quantity is the ratio of the stimulated emission rate to the spontaneous emission rate  $(e^{h\nu_{if}/k_B T} - 1)^{-1}$ . At 4 K, the  $n \rightarrow (n-1)$  transitions up to about  $n=20$ , the ratio is of the order of  $10^{-6}$  and jumps up to about  $5 \times 10^{-2}$  at  $n=30$  and becomes  $\sim 0.4$  at  $n=40$ . Substantial contribution to this ratio comes from the transitions between the lowest energy states of different  $m$  manifolds. To see the effect of the black body radiation on the decay times, we used the rate in Eq. (30) and found that the time needed to populate the ground state changed by less than 10% for  $n < 40$ . We conclude that the black body radiation will not qualitatively affect the radiative cascade for  $n < 40$ .

#### F. Semiclassical treatment

The time averaged classical power over one orbit emitted from an electron in a circular orbit with radius  $r$  in SI units is given by [17]

$$I = \frac{2}{3} \frac{e^2}{4\pi\epsilon_0 c^3} |\ddot{\vec{r}}|^2 = \frac{2}{3} \frac{e^2}{4\pi\epsilon_0 c^3} \left(\frac{v^2}{r}\right)^2, \quad (33)$$

where  $v$  is given by Eq. (23) and  $r$  is given by the Bohr-Sommerfeld quantization condition

$$m\hbar = m_e v_m r_m - \frac{eB_0 r_m^2}{2} = \pm r_m \sqrt{\left(\frac{eB_0 r_m}{2}\right)^2 + \frac{ke^2 m_e}{r_m}}. \quad (34)$$

The canonical angular momentum is  $L_z = m\hbar$  and  $\pm$  indicates the sign of  $m$ .

Energy of the orbit is obtained by

$$E = \frac{1}{2} m_e v_m^2 - \frac{e^2}{4\pi\epsilon_0 r_m} \quad (35)$$

and the semiclassical decay rate is evaluated as  $\Gamma_m = I_m / \hbar (v_m^{(\pm)} / r_m)$  where the  $\pm$  again indicates the sign of  $m$ . Note that this semiclassical treatment is only for the circular states, i.e., the high- $|m|$  states of a given  $n$  manifold. Therefore the only allowed transitions are  $n \rightarrow (n-1)$  transitions and the ground state does not decay.

Comparing the rates calculated semiclassically with the fully quantal rates in a 4.0 T field we saw that at  $n=10$  the

quantal rate is larger by  $\sim 11\%$ , at  $n=20$  by  $\sim 4\%$ , and at  $n=30$  by less than 1%. Similar errors were found for other field strengths.

We can use this semiclassical method to estimate the relative size of the decay rate due to the cyclotron motion compared to the decay rate due to the magnetron motion. For example, the cyclotron decay rate in a 1.0 T field is  $\sim 1$  Hz for the  $n=3$  state which corresponds to 4 K. The decay rate of the  $m=-85$  state due to the magnetron motion is also of the same size.

An important question is whether guiding center atoms with  $m \ll -1$  can be trapped using magnetic field gradients. The change in the energy of the circular states as a function of the magnetic field strength is an indication of the affinity of the state to a magnetic field gradient. For the purposes of trapping Rydberg atoms using magnetic field gradients, the internal energies of the atoms must increase with increasing magnetic field strength. To see if the atom is a high field or low field seeker we have approximated the motion of the electron in the orbit as a superposition of a cyclotron motion and a magnetron motion. The force on the center of mass of an atom is  $\vec{F} = -(\vec{\nabla} B)(dE/dB)$  when it is slowly moving and has internal energy  $E$ . For an electron in a central potential  $dE/dB = (e/2)\hat{B} \cdot (\vec{r} \times \vec{v})$ . We computed this quantity for the circular states in this semiclassical approximation and compared it to the  $dE/dB$  for pure cyclotron motion which is  $E/B$ . In a 1.0 T field,  $dE/dB$  is  $-24$  K/T for  $m=-85$  and is  $-20$  K/T for  $m=-125$ . The comparable values in a 3.0 T field are  $-14$  K/T and  $-12$  K/T. The magnetron motion leads to high field seeking character.

To trap the antihydrogen atoms in a spatially dependent magnetic field which is stronger near the wall of the container, one needs the atoms to be low field seekers. The  $dE/dB$  for the magnetron motion can be counteracted by the cyclotron motion. The  $dE/dB$  for pure cyclotron motion at 4 K in a 1.0 T field is 4 K/T; this is a factor of 6 smaller in magnitude than for the magnetron motion at  $m=-85$  and of opposite sign. Thus the contribution from the cyclotron motion into the low field seeking character of the atom is much smaller than the contribution into the high field seeking character of the atom from the magnetron motion. Hence we can conclude that either a lot of energy must be put into the cyclotron motion if the atoms are in circular negative  $m$  states or the atoms cannot be in nearly circular negative  $m$  states to be able to be trapped by the spatially dependent magnetic field.

#### IV. CONCLUSIONS

We have investigated the radiative cascade of highly excited hydrogen atoms in strong magnetic fields up to 4.0 T where we have considered states up to effective  $n \sim 30-35$ . We have considered two different cases of initial distributions. In one case, the states were equally populated within a small energy range and in the other case only the states with  $|m| \sim n$  are populated. We have found that in the completely random  $l, m$  case the time needed to populate the ground state by 10% is longer than the time it would take the anti-



hydrogen atoms in recent experiments to hit the walls of the container due to their thermal speed. We have also shown that the experimentally reported black body radiation at 4 K did not affect the rates and the times needed to cascade down to the ground state by more than a few percent which suggests that the black body radiation will not be of much help in getting the antihydrogen atoms to the ground state faster. This also means that it cannot slow down the cascade process by means of photoabsorption either.

Both in the completely random  $(l, m)$  distribution and the  $|m| \sim n$  distribution we see that states up to about  $n \sim 20$  are not affected much by the magnetic field as would be expected considering the atomic unit of the magnetic field being of the order of  $10^5$  T, compared to the external field of a few T.

When the initial distribution only involves states with  $|m| \sim n$ , time needed to populate the ground state is found to be longer than the completely random  $l, m$  case. This results from the initial states being high- $m$  states, which are circular or almost circular, and the fact that in completely random  $l, m$  case these states comprise a smaller fraction of the population. The only allowed transitions for the circular states in the presence of the magnetic field are either  $\Delta m = 0$  or  $|\Delta m| = 1$  transitions depending on the parity change in the transition. Therefore the states with high- $|m|$  need to cascade down through smaller  $\Delta n$  transitions than those with smaller  $|m|$ . This greatly increases the decay time to the ground state from the highly excited states in the case where the cascade initiated from the negative large  $m$  states when the magnetic field points in the  $z$  direction. When started from positive large  $m$  states the magnetic field actually speeds up the cascade process since in these states the electron is sped up by the magnetic field, radiating more intensely and decaying faster. In the case of the negative large  $m$  states, the same argument can be drawn noting that this time the magnetic field slows down the electron which radiatively loses its energy at a slower rate than in the field free case. We have shown that when started from a distribution of extreme negative  $m$  states, it takes about 800 times longer for the ground state to reach 10% population level than it does for the completely random  $l, m$  distribution at  $n = 30$  in 4.0 T magnetic field.

We have also found that when the radiative cascade starts from a circular state, the semiclassical treatment we have given here does a very good job in terms of yielding the decay rates, especially for the states with effective  $n \geq 20$ . In cases where the large fraction of the atoms are in high- $|m|$  states, the old quantum theory can be used to evaluate the decay rates instead of the full quantum theory. We used this semiclassical method to estimate the decay rate due to the cyclotron motion of the electron and compare it to the rate originating from the magnetron motion of the electron in a circular orbit. We evaluated the force on the center of mass of the atom due to the magnetic field gradient and found that for the atoms to be trapped with a spatially dependent magnetic field they should be either in highly eccentric orbits or a large amount of energy must be imparted into the cyclotron motion of the electron.

## ACKNOWLEDGMENTS

This work was supported by the Chemical Sciences, Geosciences, and Biosciences Division of the Office of Basic Energy Sciences, U.S. Department of Energy.

## APPENDIX

The exact Hamiltonian for a hydrogen atom in an external magnetic field  $\vec{B} = B\hat{z}$  is

$$H = \frac{[\vec{p} - q\vec{A}(\vec{r})]^2}{2\mu} + \frac{B^2}{2M}(x^2 + y^2) + \frac{BK}{M}x - \frac{1}{r^2} + \frac{K^2}{2M}, \quad (\text{A1})$$

where  $M = m_e + m_p$ ,  $\mu = m_e m_p / M$  is the reduced mass,  $K$  is the pseudomomentum assumed to be in the  $y$  direction, and  $q = e(m_p - m_e) / M$  [18]. The Hamiltonian (2) can be obtained by making four approximations to the exact Hamiltonian. (1) We use the mass of the electron  $m_e$  instead of the reduced mass  $\mu$ . This gives a change at the  $\sim 1/1000$  level and thus is not interesting for our purposes. (2) We do not include the last term  $K^2/2M$  since this a constant and does not affect the composition of the states or their relative energies. (3) We do not include the term  $B^2(x^2 + y^2)/2M$ . This term is  $\sim 500$  times smaller than the comparable diamagnetic term in our Eq. (2) and thus does not have an important effect on our results. (4) We do not include the term  $BKx/M$ . The effect of this term is the motional Stark effect since the atom has a velocity perpendicular to the magnetic field  $\vec{B}$ . The pseudomomentum is

$$\vec{K} = \vec{P} + \frac{e}{2}\vec{B} \times \vec{r}, \quad (\text{A2})$$

where  $\vec{P} = M\vec{V}$  is the linear momentum of the proton and  $\vec{r}$  is the distance from the proton to the electron. In a 4 T field and with a kinetic energy of 4 K the first term in  $\vec{P}$  has magnitude  $\sim 4.3 \times 10^{-25}$  kg m/s while the second term  $e\vec{B} \times \vec{r}/2$  has magnitude  $\sim 1.5 \times 10^{-26}$  kg m/s. Thus we can take  $K \sim MV$  in our estimates. To see that the Stark shift does not have an important effect on our results, we note that the magnitude of the paramagnetic splitting of the levels due to the magnetic field is  $\Delta E_p^{(1)} = (B/2)|\Delta m|$  and is  $\sim 2.13 \times 10^{-6}$  a.u. in a 1 T field for the adjacent levels. The thermal speed of an antihydrogen atom at 4 K [2,3] is  $\sim 260$  m/s. An antihydrogen atom moving with a velocity  $\vec{V}$  in a magnetic field  $\vec{B}$  experiences an electric field of magnitude  $\mathcal{E} \sim |\vec{V} \times \vec{B}|$ . The correction to the energy levels in the first approximation in an  $n$ -manifold due to the linear Stark effect resulting from this field is  $E_s^{(1)} = \frac{3}{2}\mathcal{E}n(n_1 - n_2)$  where  $n_1$  and  $n_2$  are the parabolic quantum numbers [15]. The separation of the adjacent Stark levels would be  $3\mathcal{E}n$  which is  $\sim 4.5 \times 10^{-8}$  a.u. in  $n = 30$  manifold for an atom moving at 260 m/s in a 1 T field. Note that the paramagnetic splitting is larger than the Stark splitting by roughly two orders of magnitude, therefore the linear Stark effect is negligible.

Actually, the eigenvalues and eigenvectors of  $V Bx + B L_z$  can be found analytically within an  $n$  manifold. We com-

puted the average spread in  $m$  for each state in an  $n$  manifold which we defined to be  $\Delta m^2 \equiv \langle L_z^2 \rangle - \langle L_z \rangle^2$ . We averaged  $\Delta m^2$  over all of the states and found it to be  $3V^2 n^3(n+1)/4$  which is  $\sim 9 \times 10^{-3}$  for  $n=30$ . Again this shows that most states hardly mix with other  $m$ 's and the main mixing is with  $m \pm 1$ . Since each state is mixing with states of similar radiative properties, our results on radiative cascade should be accurate to better than a few percent.

Clearly, the extent to which the Hamiltonian of Eq. (2) is accurate depends on the application. For investigations of large scale and/or averaged quantities, several different estimates including comparison of the sizes of  $MV$  and  $eBr/2$  in the pseudomomentum, comparison of the proton cyclotron

frequency to the frequency of the electron in the guiding center atom, and the size of the motional Stark field to the magnetic field suggest that the Hamiltonian (2) is good enough for accuracy better than  $\sim 10\%$  for  $n \leq 60$  for  $B \leq 4$  T and kinetic energy less than 4 K.

In addition to the strong magnetic fields, antihydrogen experiments also involve spatially dependent electric fields of  $\sim 10$  V/cm which is roughly a factor of  $\sim 1-4$  times larger than the motional Stark field. Since the configurations of the traps are not known at this time, we will not speculate on the effect of these electric fields. In light of the estimates in this Appendix, it seems unlikely that these electric fields will have a substantial effect on our results.

- 
- [1] M. Amoretti *et al.*, Nature (London) **419**, 456 (2002).  
 [2] G. Gabrielse, N. S. Bowden, P. Oxley, A. Speck, C. H. Storry, J. N. Tan, M. Wessels, D. Grzonka, W. Oelert, G. Schepers, T. Sefzick, J. Walz, H. Pittner, T. W. Hänsch, and E. A. Hessels (ATRAP Collaboration), Phys. Rev. Lett. **89**, 213401 (2002).  
 [3] G. Gabrielse, N. S. Bowden, P. Oxley, A. Speck, C. H. Storry, J. N. Tan, M. Wessels, D. Grzonka, W. Oelert, G. Schepers, T. Sefzick, J. Walz, H. Pittner, T. W. Hänsch, and E. A. Hessels (ATRAP Collaboration), Phys. Rev. Lett. **89**, 233401 (2002).  
 [4] R. Bluhm, V. A. Kostelecký, and Neil Russell, Phys. Rev. Lett. **82**, 2254 (1999).  
 [5] T. Udem, A. Huber, B. Gross, J. Reichert, M. Prevedelli, M. Weitz, and T. W. Hänsch Phys. Rev. Lett. **79**, 2646 (1997).  
 [6] C. L. Cesar, D. G. Fried, T. C. Killian, A. D. Polcyn, J. C. Sandberg, I. A. Yu, T. J. Greytak, D. Kleppner, and J. M. Doyle, Phys. Rev. Lett. **77**, 255 (1996).  
 [7] G. Gabrielse, S. L. Rolston, and L. Haarsma, Phys. Lett. A **129**, 38 (1988).  
 [8] F. Robicheaux and J. D. Hanson, Phys. Rev. A **69**, 010701(R) (2004).  
 [9] F. Robicheaux, Phys. Rev. A **73**, 033401 (2006).  
 [10] J. R. Guest and G. Raithel, Phys. Rev. A **68**, 052502 (2003).  
 [11] J. R. Guest, J.-H. Choi, and G. Raithel, Phys. Rev. A **68**, 022509 (2003).  
 [12] M. R. Flannery and D. Vrinceanu, Phys. Rev. A **68**, 030502(R) (2003).  
 [13] When  $2n^2 \ll r_f$ , the  $\epsilon_{nl} = -1/(2n^2)$  are the usual field free energy levels. In the opposite limit, the  $\epsilon_{nl}$  rapidly increase to be greater than zero and have the form  $C_l + \pi^2(n-D_l)^2/(2r_f^2)$ , where  $C_l$  and  $D_l$  are constants that depend on  $l$  and  $r_f$ .  
 [14] C. W. Clark and K. T. Taylor, J. Phys. B **15**, 1175 (1982).  
 [15] L. D. Landau and E. M. Lifshitz, *Quantum Mechanics*, 3rd ed. (Pergamon Press, Noida, 1998).  
 [16] R. D. Cowan, *The Theory of Atomic Structure and Spectra*, 3rd ed. (University of California Press, Los Angeles, 1981).  
 [17] J. D. Jackson, *Classical Electrodynamics*, 3rd ed. (Wiley, New York, 1998).  
 [18] O. Dippel, P. Schmelcher, and L. S. Cederbaum, Phys. Rev. A **49**, 4415 (1994).